Structure of the Detergent Phase and Protein–Detergent Interactions in Crystals of the Wild-Type (Strain Y) *Rhodobacter sphaeroides* Photochemical Reaction Center

M. Roth,*,‡ B. Arnoux,§ A. Ducruix,§ and F. Reiss-Husson∥

Laboratoire d'Ingénierie des Protéines, LIP/LCCP, Centre d'Etudes Nucléaires de Grenoble, BP 85X, 38041 Grenoble Cedex, France, Institut de Chimie des Substances Naturelles, CNRS, and CNRS, UPR407, 91198 Gif-sur-Yvette Cedex, France

Received March 14, 1991; Revised Manuscript Received June 26, 1991

ABSTRACT: *Rhodobacter sphaeroides* (strain Y) reaction center (RC) crystals were grown in the presence of *n*-octyl β-glucoside (β-OG). In order to determine the structure of the detergent phase in these crystals, low-resolution neutron diffraction experiments were performed at different contrasts obtained by varying the H_2O/D_2O ratio in the solvent. From the contrast variation data and from the RC atomic coordinates determined by X-ray diffraction [Arnoux, B., Ducruix, A., Reiss-Husson, F., Lutz, M., Norris, J., Schiffer, M., & Chang, C. H. (1989) *FEBS Lett. 258*, 47–50], a model was obtained for the structure of the detergent phase in the crystal. The detergent forms a ring-shaped micelle surrounding the most hydrophobic part of the transmembrane α helices of the RC. Each detergent ring is connected to two next-neighbor rings by intermicellar bridges. The detergent phase is organized thus in infinite zigzag chains parallel to the *b* axis of the $P2_12_12_1$ unit cell. The main interactions between β-OG molecules and the RC molecules are hydrophobic and are localized at the level of the transmembrane α helices. This interaction replaces the phospholipid–protein interaction existing in vivo in the membrane and, to some extent, also the light harvesting complex–protein interaction. Secondary hydrophilic interactions are found between a few of the charged residues of the H subunit and the hydrophilic surface of the detergent ring from a neighboring RC molecule. A comparison with a previous study on *Rhodopseudomonas viridis* crystals [which grow in the presence of lauryldimethylamine *N*-oxide (LDAO) and belong to a different space group] [Roth, M., Lewit-Bentley, A., Michel, H., Deisenhofer, J., Huber, R., & Oesterhelt, D. (1989) *Nature 340*, 659–661] shows a quasi identity of shape and position of the β-OG and LDAO rings around the transmembrane α helices. The secondary interactions, involving in both cases the external surface of the H subunit, differ because of the different molecular packing in the two space groups. The role and structural requirements of the detergent in the crystallization process are discussed.

Membrane proteins can be solubilized in the presence of a suitable detergent that perturbs the lipid and protein interactions, breaks down the membrane structure into smaller entities, and finally releases the protein components as discrete protein–detergent complexes. It is generally assumed that in these complexes the protein is surrounded by a "belt" of detergent molecules that covers the hydrophobic regions originally embedded in the membrane. Such a view gained support from small-angle scattering studies in detergent solution of rhodopsin (Sardet et al., 1981; Osborne et al., 1978) and Ca^{2+}-ATPase (le Maire et al., 1981). These studies were, however, unable to give a precise description of the shape and size of the region occupied by the detergent. A commonly expressed view was that the protein is inserted in an ellipsoidal micelle whose shape is roughly the same as that in the absence of protein (Robinson & Tanford, 1976). Alternatively, it was proposed that the detergent is located in a monolayer around the hydrophobic domain (le Maire et al., 1983).

Recently, the localization of LDAO[1] detergent around the photosynthetic reaction center molecule from *Rhodopseudomonas viridis* was described by using low-resolution diffraction of reaction center crystals (Roth et al., 1989). Except for a single ordered LDAO molecule that was localized in the high-resolution X-ray structure (Deisenhofer & Michel, 1989a,b), the detergent is disordered and can be seen only at low resolution with contrast variation, a method conveniently performed by neutron diffraction in H_2O/D_2O buffer. Thus LDAO is shown to be concentrated in rings around the transmembrane helices of the reaction center subunits L, M, and H. The detergent rings appear to be interconnected into infinite zigzag chains. The bulky cytochrome subunit and most of the cytoplasmic part of the H subunit are devoid of detergent; they are involved in the protein–protein contacts responsible for the packing in the lattice. Remarkably, the thickness of the detergent rings is slightly smaller than the total length of the transmembrane α helices, leaving part of these helices exposed to the solvent toward the cytoplasmic side.

In this work, we extend this approach to localize another detergent, β-OG, in crystals of *Rhodobacter sphaeroides* strain Y reaction centers, the structure of which was recently determined by X-ray diffraction (Arnoux et al., 1989). Unlike the *Rps. viridis* reaction center, the *Rb. sphaeroides* reaction center is composed only of the L, M, and H subunits and their associated pigments and cofactors. Thus the hydrophobic character of the protein from *Rb. sphaeroides* is more pronounced. Its packing in the crystal lattice (Chang et al., 1986; Arnoux et al., 1990) is also different. In addition, β-OG belongs to another detergent class than LDAO, with a different

* To whom correspondence should be addressed.
‡ Centre d'Etudes Nucléaires de Grenoble.
§ Institut de Chimie des Substances Naturelles, CNRS.
∥ UPR407, CNRS.

[1] Abbreviations: LDAO, lauryldimethylamine oxide; β-OG, *n*-octyl β-D-glucoside; HPTH, heptane-1,2,3-triol; *Rps.*, *Rhodopseudomonas*; *Rb.*, *Rhodobacter*; B875 and B1020 LHCI, light harvesting complexes I with absorption maxima at 875 and 1020 nm, respectively.

0006-2960/91/0430-9403$02.50/0

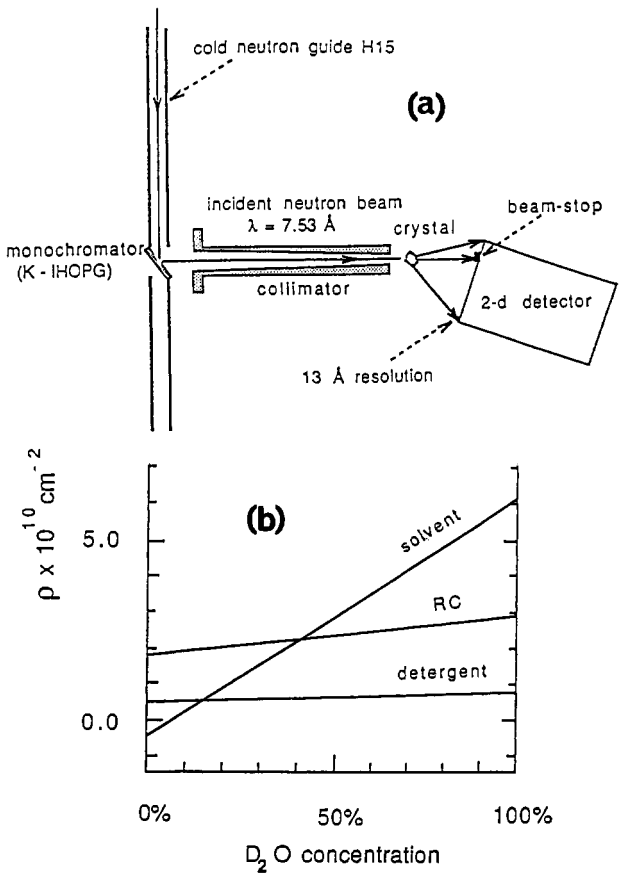

FIGURE 1: (a) Schematic representation of the experimental setup for low-resolution neutron diffraction at the Institut Laue-Langevin. The monochromator is a K-intercalated highly oriented pyrolytic graphite crystal. The size of the beam cross section is about 30 × 30 mm² at the entrance of the collimator and has a diameter of 1 mm at the exit. The collimator length is 1 m. The sample-to-detector distance used was 25 cm. The area of the 2-D position-sensitive detector is about 20 × 20 cm², with a matrix of 128 × 128 pixels. (b) Scattering length density calculated for protein + chromophores (straight line marked RC), detergent, and solvent, as a function of D_2O concentration in water (see Appendix). The intersections of the straight lines give the D_2O concentrations corresponding to the theoretical isopycnic points of detergent (near 18.7%) and protein + chromophores (near 40%) with respect to solvent.

hydrophilic–hydrophobic balance due to its shorter hydrocarbon chain (C_8 versus C_{12}) and its bulkier polar head group. The critical micellar concentration of β-OG in water is quite high [25 mM (Suarez et al., 1984)] as compared to LDAO [2 mM (Hermann, 1962)], which is indicative of a greater mobility of the β-OG molecules. It seems thus of interest to determine the localization of β-OG in the unit cell and its interactions with *Rb. sphaeroides* reaction centers and to compare these findings with those obtained previously for LDAO in *Rps. viridis* reaction centers.

Materials and Methods

Materials. Reaction centers from *Rb. sphaeroides* strain Y were purified with the detergent LDAO as previously described (Rivas et al., 1980). The reaction centers were freed of bound LDAO by extensive dialysis at 5 °C against a 10 mM Tris-HCl buffer, pH 8.0, containing 1 mM EDTA and 0.1% (w/v) sodium azide, until precipitation occurred. The dialysis buffer was then exchanged for a buffer of the same composition but containing 0.8% (w/v) β-OG, and dialysis was performed for 24 h. LDAO was obtained from Fluka and β-OG from Bachem; poly(ethylene glycol) 4000 (Merck) was purified before use (Ray & Puvathingal, 1985).

Table I: Intensity-Merging *R*-Factors R_{sym}[a]

	resolution range			
contrast (%)	$d < 20$ Å	$20 < d < 30$ Å	$d > 30$ Å	cumulated
0	42.8	15.7	1.9	8.5
33	53.9	25.8	2.1	14.1
66	30.4	6.1	1.5	3.6
100	79.8	18.3	3.4	10.9

[a] R_{sym} is defined as usual by

$$R_{sym} = \frac{\sum_{hkl}(\sum'_{h'k'l'}|I(h'k'l') - \langle I(hkl)\rangle|)}{\sum_{hkl}\sum'_{h'k'l'} I(h'k'l')}$$

and is calculated by taking into account all reflections of the data set. The sum $\sum$ is made over all unique indices $[hkl]$ and $\sum'$, over all $[h'k'l']$ equivalent to $[hkl]$ in the space group, and $\langle I(hkl)\rangle$ is the sample average of the equivalent intensities $I(h'k'l')$. The values of R_{sym} are given in percent. The contrast is given in percent of D_2O in the solvent water.

Crystallization. Crystallization was performed by microdialysis in sealed capillaries as described by Ducruix and Reiss-Husson (1987). Samples of 40 μL, containing 2 mg/mL protein in 15 mM Tris-HCl buffer, pH 8.0, 1 mM EDTA, 0.1% (w/v) sodium azide, 0.8% (w/v) β-OG, 6.5% (w/v) PEG 4000, and 0.11M NaCl, were equilibrated at 18 °C against a reservoir containing 13% (w/v) PEG 4000 and 0.22 M NaCl in the same 15 mM Tris-HCl, 1 mM EDTA, 0.1% (w/v) sodium azide, and 0.8% (w/v) β-OG buffer, pH 8.0. Orthorhombic crystals grew as long rods with a diamond-shaped cross section (space group $P2_12_12_1$; unit cell parameters a = 143.7 Å, b = 139.8 Å, c = 78.65 Å). The diffraction experiments were performed at four different D_2O/H_2O concentrations, i.e., four contrasts; these were obtained by dialyzing the crystals in their microdialysis capillaries for 1 month, in a buffer of the same composition as the crystallization reservoir but with a different D_2O/H_2O concentration [0%, 33%, 66%, and 100% D_2O (v/v)]. Crystals of approximately 1.5 × (0.3–0.4) × 0.2 mm³ were selected for the experiments.

Neutron Diffraction Experiments. (A) Data Collection. Neutron diffraction data were collected on the instrument DB21 at the Institut Laue-Langevin (Grenoble, France) at a fixed neutron wavelength, λ = 7.53 Å, on a four-circle diffractometer, with a two-dimensional (200 × 200 mm²) position-sensitive scintillation detector of Anger camera type (Roche et al., 1985) with 2.0-mm resolution, set at 250 mm from the crystal. Data sets were collected in normal beam geometry, with one fixed position of the detector (Figure 1a). The measuring time of a full data set at 13-Å resolution varied from 1 to 3 weeks depending on the contrast.

(B) Data Evaluation. The diffraction reflections were integrated by using the set of programs developed by A. Lewit-Bentley, G. A. Bentley, and M. Roth at ILL and EMBL (Grenoble Outstation) (Roth & Lewit-Bentley, 1986). The results, in terms of overall merging *R*-factors, R_{sym}, are of good quality at a resolution lower than 20 Å ($d > 20$ Å), as indicated in Table I. At higher resolution, the accuracy of the data is low. This is related to the weakness of the neutron Bragg diffraction with respect to background in the high-resolution range, not to the quality of the crystals [which diffracted with X-rays at 3-Å resolution; see Arnoux et al. (1989)]. The 33% D_2O data are the less accurate for the following reason. In H_2O/D_2O contrast variation diffraction experiments, the total intensity diffracted in all spots at low resolution varies parabolically as a function of the D_2O concentration [see, for instance, Roth (1987)]. In a system constituted by two components (in our case, by protein and detergent), the contrast corresponding to the minimum of the

Table II: Statistics on Data Set Scaling[a]

contrast (%)	F's scale factor	std dev
0	1.000	
33	0.889	0.055
66	0.631	0.027
100	2.96	0.13

[a] Number of reflections measured in at least three contrasts at 13-Å resolution: 370, including 109 very weak reflections without useful contrast variation information about the phase angle. Total number of reflections at 13-Å resolution: 470. Completeness: 79%. The contrast is given in percent of D_2O in the solvent water.

parabola is located somewhere between the scattering length density isopycnic points of the two components with respect to the solvent, i.e., between 10% (see discussion below) for detergent and 40% for protein (see Figure 1b). Therefore, the diffraction at 33% is weaker than at the other contrasts we measured. The diffraction data were not corrected for absorption because during data collection the neutron beam was almost always perpendicular to the long axis of the elongated crystals (which is parallel to the crystallographic *a* axis).

The relative scaling of the four data sets was made by using a least-squares technique based on the linearity of the complex structure factors with respect to the contrast, i.e., with respect to the D_2O concentration of the solvent (Roth et al., 1984); see Table II. The number of unique reflections measured in at least three contrasts (one needs data from at least three different contrasts to get phase angle information from contrast variation experiments) was 370 at 13-Å resolution, constituting a data set of nearly 80% completness.

Structure Determination

From low-resolution neutron diffraction studies on the *Rps. viridis* reaction center crystals, it is known that the detergent is segregated into a detergent-rich phase well separated from an aqueous phase depleted in detergent. These two phases are called hereafter "detergent phase" and "solvent", respectively. The structure determination consists of delineating the shape of the detergent phase, by analyzing and interpreting density maps calculated at an appropriate contrast. The phase angles of the measured structure factors necessary for calculating the density maps were calculated by combining the phase angle information contained in the contrast variation data and the phase angle information obtained from the known position and structure of the protein and the prosthetic groups in the unit cell. The phasing is improved progressively by modeling the detergent phase in an iterative way (see below).

The method used for combining, on a statistical basis, calculated structure factors of a model on one side, and F_o and phase angle differences from the contrast variation data on the other, was proposed by Roth (1987, 1990). The aim of this algorithm (called hereafter "BESF" algorithm, for best estimate structure factors algorithm) is to calculate the expectation value of structure factors of the system, having given as input, first, the structure factors of the current model and their statistical probability distribution, calculated in different contrasts, and, second, the contrast variation data with their statistical distribution. These expectation values are best estimate structure factors because they result from the minimization of a cost function expressed as the sum of square density errors (Blow & Crick, 1959; Roth, 1987).

The method used for modeling the detergent phase from a density map consists of a smoothed three-dimensional contouring of the density regions selected as belonging to the detergent phase.

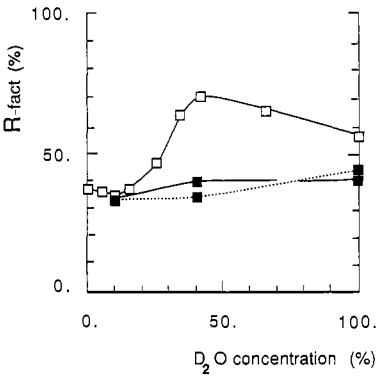

FIGURE 2: *R*-factor of calculated structure factors with respect to observed structure factors F_o (relation 2) at different D_2O contrasts: (a) (□) with structure factors calculated with the RC molecule alone, before modelization of the detergent phase; (b) (■) with structure factors calculated after detergent-phase structure refinement, with and without final smoothing of the detergent-phase model (solid and dotted lines, respectively).

The detergent-phase structure determination proceeds in four steps:

Preliminary Step: Search for the Contrast of Least Contribution of Detergent to Diffraction. This search is achieved by determining the contrast where the agreement is the best between the measured structure factors F_o and the moduli of the structure factors F_{RC} calculated with the molecular complex protein plus prosthetic groups (call "RC" molecule hereafter) alone.

The structure factors F_{RC} are calculated, at the absolute scale, in different contrasts, according to the formula:

$$F_{RC}(hkl) = \sum_{i=1}^{N}(B_i - \rho_{solvent}V_i)e^{-4\pi^2 s^2 R_i^2/6}e^{-i\pi s r_i} \quad (1)$$

Relation 1 is calculated by dividing the RC molecule into N small atom groups (for the polypeptides, it is natural to use as groups the amino acid residues; for the prosthetic molecules, we used groups of about 12 neighboring atoms); then the total scattering length B_i of each group is calculated (by adding the scattering length of each individual atom), together with its volume V_i, typically of the order of 5 Å^3 (Worcester, 1976; Jacrot, 1976), and its average radius of gyration R_i. s is the scattering vector corresponding to the reflection $[hkl]$ and r_i the position of the center of mass of the scattering length density of the atomic group i in the unit cell. All these quantities can be calculated when the structure of the RC molecule and the chemical composition of the solvent are known.

Structure factors F_{RC} are compared to the corresponding measured F_o values by using the conventional *R*-factor, calculated for F_o values larger than 2σ:

$$R = \sum_{hkl}|S|F_c| - F_o|/\sum_{hkl}F_o \quad (2)$$

with $\sum_{hkl}$ limited to $F_o(hkl) > 2\sigma(F_o)$ and $F_c = F_{RC}$, S being the scale factor.

For contrasts where data were not effectively recorded, the corresponding F_o values were obtained from a linear interpolation as a function of the contrast, in the complex plane, of the measured values (Roth et al., 1984). The atomic coordinates of the *Rb. sphaeroides* strain Y RC molecule we used were refined by Arnoux et al. (1989), starting from the coordinates of the R26 mutant communicated by Chang et al. (1986).

The calculation of $\rho_{solvent}$ is detailed in the Appendix; it is a linear function of the D_2O concentration of the solvent water.

The scattering lengths B_i are also linear functions of this concentration for all residues which have one or several H atoms exchangeable with the H atoms of water.

At this stage, before modeling, the best R-factor agreement for *Rb. sphaeroides* crystal data is found near a concentration of 10% D_2O in solvent water with a value of $R \approx 34.6\%$ (see Figure 2), indicating that this is the contrast at which the detergent is contributing the least to the diffraction. This result is in disagreement with the value of 18.7% D_2O determined by theoretical contrast calculations for the scattering length isopycnic point between β-OG and solvent (see Appendix and Figure 1b). At 18.7% D_2O contrast, the value of R is about 40%. This discrepancy can be due to nonuniformity of the scattering length density of the detergent phase: the scattering length density of the alkyl chains of the detergent molecules is much smaller (close to the 0% D_2O solvent scattering length density) than that of the head groups, and it is very likely that the former occupy mostly one side of the detergent phase (the side in hydrophobic contact with the protein) and the later the other side (the solvent side).

Step 1: Determination of a First Model of the Structure of the Detergent Phase. First Application of the BESF Algorithm. The calculation is made by using, as input, the model structure factors F_{RC} of RC molecules alone, calculated at two contrasts, 10% D_2O and 100% D_2O. The first contrast is chosen because of the weakness of the detergent-phase contribution to diffraction. The second because, at this contrast, (1) the detergent phase and RC molecule have good contrasts with respect to solvent, therefore contributing equally well to diffraction, and (2) the phase angles of the partial structure factors F_{RC} and the phase angles of the full structure factors (RC + detergent phase) are similar.

Using the BESF algorithm, we calculated a best density map at 40% D_2O contrast. At this contrast, the contribution of the detergent to the diffraction is predominant. From this density map, a first model of the detergent structure at low resolution is derived.

Low-Resolution Structure Modeling of the Detergent Phase. The method of delineating and modeling the detergent phase from a low-resolution density map is a simple density treatment of the map, having discarded the density corresponding to the known part of the structure. As a byproduct, this density treatment reduces the noise level of the map, like any solvent-flattening technique does. The calculation could in principle be carried out at any contrast. At 40% D_2O contrast, however, the detergent-phase contouring is least biased by phasing and termination errors related to the protein density because the protein density is there at its lowest contrast with respect to the solvent density. As a prerequisite, one needs to know the volume f_{det} of the phase to be modeled. The part of the density map to be discarded is defined by its envelope.

(*A*) *Molecular Envelope.* The envelope of the RC molecule was calculated from the density map of the molecule at 100% D_2O. At this concentration, both protein and prosthetic groups have high negative contrast with respect to the solvent. It was made by contouring the Fourier density map at a level such to enclose a volume equal to the estimated volume of the RC molecule (~32% of the unit cell volume in our case).

(*B*) *Modeling.* The density map treatment is illustrated on Figure 3 and proceeds as follows:

(1) The molecule density, i.e., the density inside the molecular envelope, is replaced by a constant flat solvent density $\rho_{solvent}$.

(2) The histogram of the density map outside the molecular envelope is then calculated, and from this histogram the density level ρ_1 giving the expected volume for the detergent phase

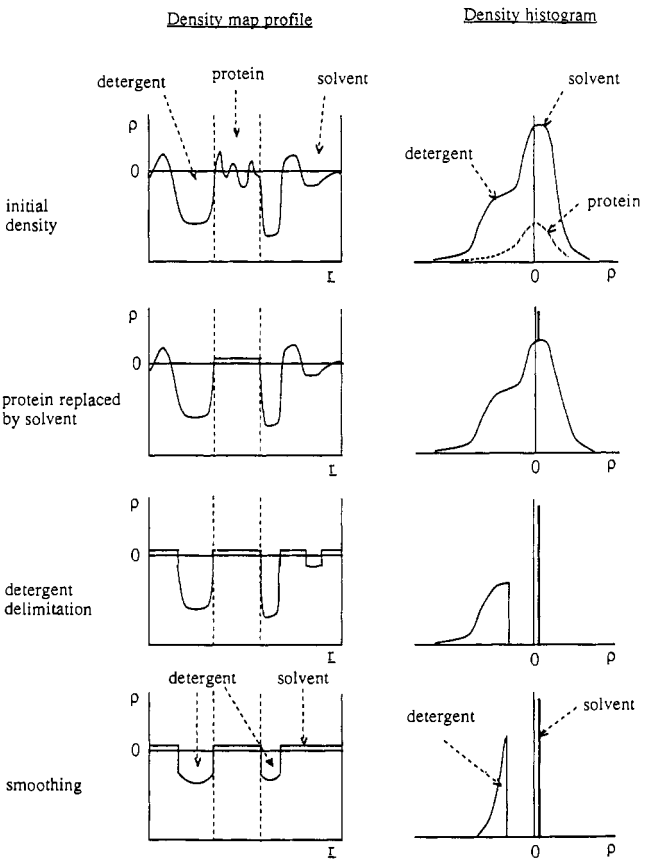

FIGURE 3: Schematic illustration of the method of modeling the detergent phase from a density map, as described under Low-Resolution Structure Modeling of the Detergent Phase.

is determined. At 40% D_2O, the density of the detergent is negative with respect to solvent; therefore, the pixels belonging to the detergent phase are on the negative side abscissa of the histogram.

(3) The pixels having density higher than ρ_1 are leveled to solvent density $\rho_{solvent}$; the density of the other pixels is kept unchanged. The value of $\rho_{solvent}$ is given by the abscissa of the peak of the histogram.

(4) The resulting density map is smoothed by weighted local density averaging in a way similar to solvent-flattening method of Wang (1985): the density of each pixel of the map is replaced by an average of its own density value and of the weighted density of the neighboring pixels. We used weighting coefficients decreasing linearly with distance, with a cutoff radius of typically two pixel sizes, i.e., 10 Å. The effect of this treatment is to smooth to some extent the shape of the interface between the detergent phase and solvent by eliminating from the density map short-range oscillations and noise.

(5) Repeating operation 2 leads to a new value of ρ_1 and repeating operation 3, to a new solvent flattening. The smoothed detergent-phase model is constituted by all pixels having a density lower than ρ_1. Having calculated the average density ρ_{det} of these pixels, one replaces finally the actual value of their density by this average value.

The final output of this treatment is thus a two-level density map constituting the detergent-phase model.

Step 2: Refinement of the Structure of the Detergent Phase. Iterative Application of the BESF Algorithm and Detergent Modeling. The calculation is made by using, as input, model structure factors corresponding to a tentative complete model of the structure made by associating the RC molecule and the detergent-phase model. Calculated structure factors at three contrasts, 10%, 40% and 100% D_2O, are used. Again, best

Table III: *R*-Factor Values during Modeling and Refinement Process[a]

	contrast		
	10% D_2O	40% D_2O	100% D_2O
initial value, with RC molecule alone	34.6	69.3	59.7
RC + first model of detergent phase (step 1)	32.2	45.3	47.3
RC + detergent-phase model at the end of step 2	33.3	44.4	38.8
RC + detergent-phase model at the end of step 3 with a smoothed model of detergent (9-Å smoothing radius)		40.2	40.5
RC + detergent-phase model at the end of step 3 without smoothing		33.2	43.2

[a] The table shows the evolution of the *R*-factor value (given in percent and defined by relation 2) between the calculated structure factors of the complex model constituted by protein plus chromophores (RC) and the detergent phase and the measured structure factors F_o, at successive steps of the process of refinement of the shape of the detergent phase. The steps of refinement are described under Structure Determination. The introduction of the detergent phase in the model of the complex produces a marked drop in the *R* values as well as the refinement of its shape. The final *R*-factor value depends somewhat on the degree of smoothing applied during modeling. For the 10% D_2O contrast, which is close to the contrast matching point of the detergent with respect to the solvent, the *R* values are not strongly modified by the detergent-phase refinement.

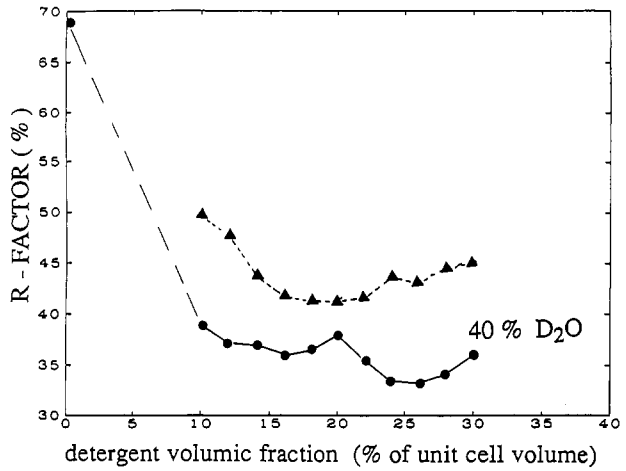

FIGURE 4: Variation of the *R*-factor value as a function of the relative detergent volume in the lattice, f_{det}, used in the modeling of the detergent phase at 40% D_2O. This *R*-factor search corresponds to the last step (step 3) of structure refinement, modeling of detergent phase without (●) and with (▲) smoothing, respectively.

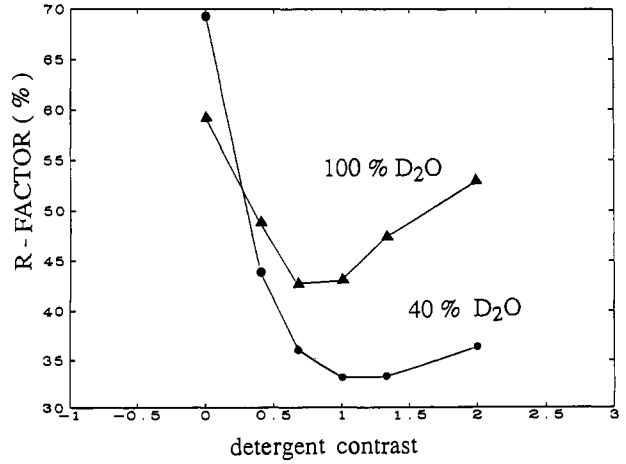

FIGURE 5: *R*-factor search of the best contrast ρ_s between the detergent phase and the solvent, at two different D_2O concentrations in solvent water. The contrast (abscissa) is represented by its relative value $\rho_s/\rho_{solvent}$, with respect to the theoretical value $\rho_{solvent}$ at the two D_2O concentrations. These theoretical values are calculated on the assumption that there is no detergent in the solvent and no water in the detergent phase (see Appendix).

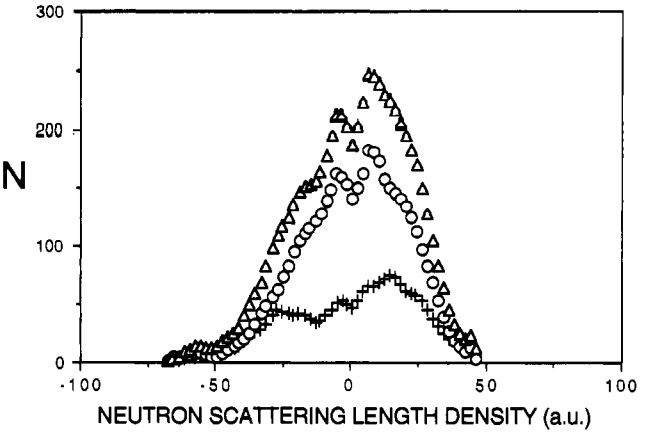

FIGURE 6: Histogram of *N*, the number of density map pixels per density interval at 40% D_2O, after the first best density map determination (step 1 of the structure refinement): (△) histogram of the whole map; (+) histogram of the map inside the RC molecule envelope; (○) histogram of the map outside the RC molecule envelope.

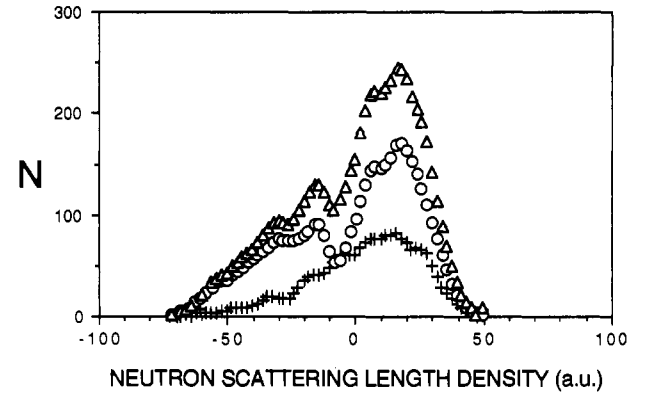

FIGURE 7: Histogram of pixel density of the density map at 40% D_2O contrast, after the last best density map determination (end of refinement); same symbols as in Figure 6.

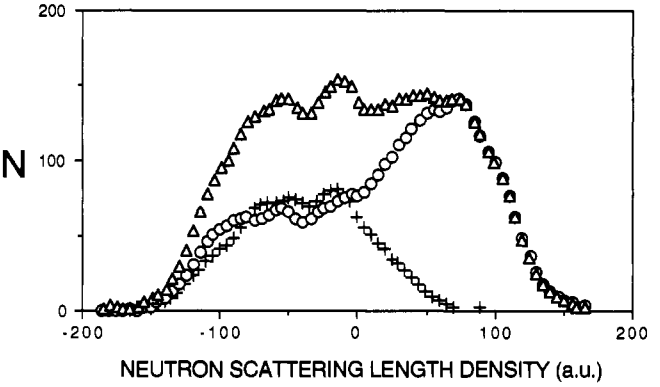

FIGURE 8: Same as Figure 7 at 100% D_2O.

estimates of the structure factors at contrast 40% D_2O are determined. A new detergent-phase model is derived from the corresponding density map with the method described above. And this is repeated iteratively to improve the detergent-phase model progressively.

The combination of the detergent-phase model and the RC model is made in reciprocal space. The structure factors of the model are calculated with relation 1. The structure factors of the detergent phase are calculated by reverse fast Fourier transform of the detergent-phase model. A relative scaling factor α between both structure factors, adjusted by least squares, is used according to

$$F_{total} = F_{RC} + \alpha F_{det} \quad (3)$$

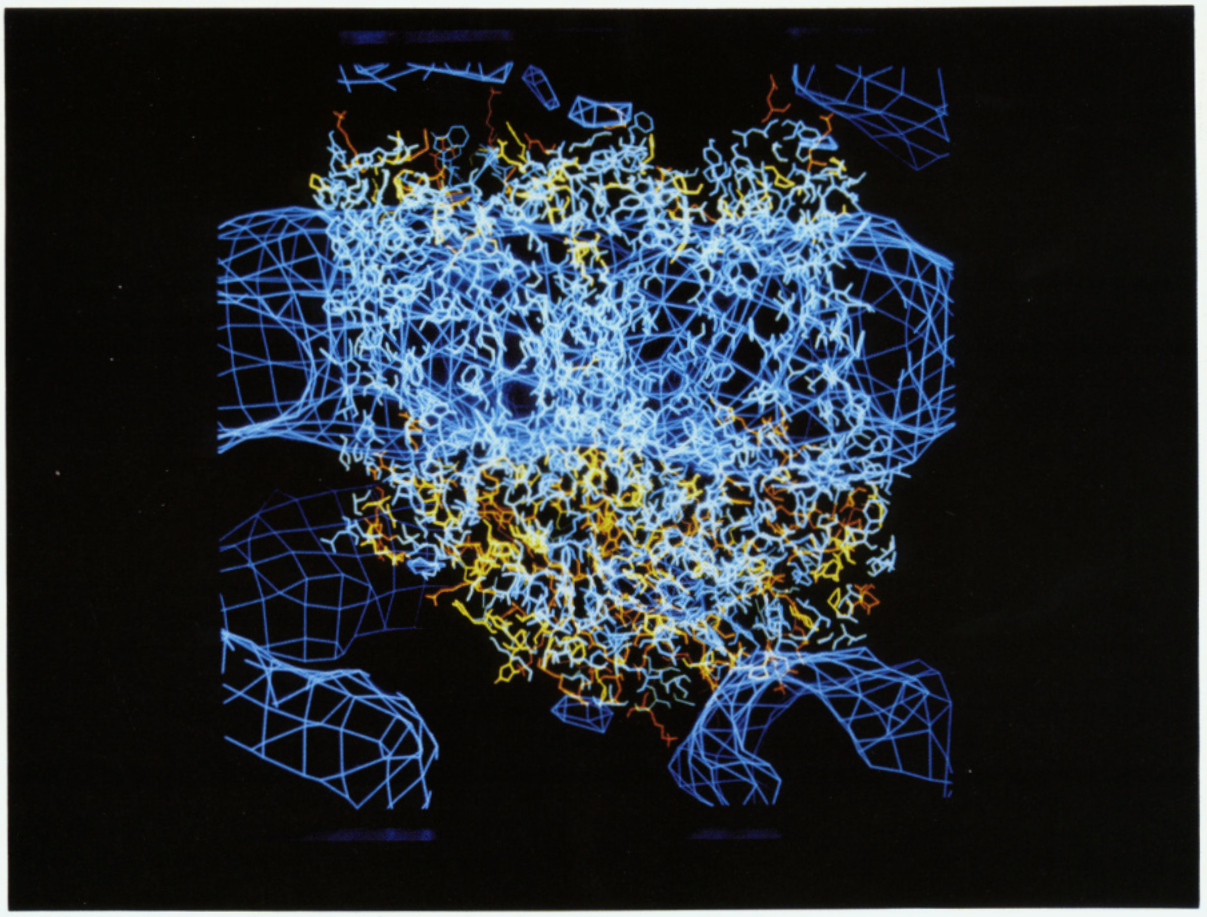

FIGURE 9: View of an RC molecule with its detergent-phase ring with a color coding of the amino acid residues (from blue to red) according to the following hydrophobic scale: blue, Phe, Met, Ile, Leu, Val, Cys, Trp, Tyr; light blue, Ala, Gly, Thr, Ser; yellow, Pro, His, Gln, Asn; orange, Glu, Asp, Lys, Arg. The vertical axis of this picture is nearly parallel to the transmembrane axis of the molecule. This view shows that the detergent-phase ring is located exactly at the height of a more or less median region of subunits L and M, which appears completely devoid of polar and charged residues, and thus represents very likely the transmembrane region of the RC molecule. This detergent ring and the region of the detergent phase below which interacts with the H subunit belong to two different parallel detergent ring chains.

and the sum is scaled against the data by a global scaling factor s_c:

$$s_c|\boldsymbol{F}_{total}| = F_o \tag{4}$$

The two parameters, s_c and α, are determined by least squares, by minimizing the quantity

$$\sum_{hkl}(s_c|\boldsymbol{F}_{RC} + \alpha\boldsymbol{F}_{det}| - F_o)^2 \tag{5}$$

The iteration is continued until the best agreement is found between $s_c|\boldsymbol{F}_{total}|$ and F_o. This is achieved usually in five to six iterations.

Step 3: *Determination of the Volume Occupied by the Detergent Phase in the Unit Cell and Its Contrast with Respect to Solvent*. Up to this point, the refinement is carried out with a reasonable tentative a priori value of the volume f_{det} occupied by the detergent phase in the unit cell. In our case the value was 30%. A better estimate of this parameter was then searched by the following method: starting from the structure model obtained at the end of step 2, the refinement is continued in the same iterative way except that the structure factors of the model RC plus detergent phase are calculated without the adjustable relative scale factor α:

$$\boldsymbol{F}_{total} = \boldsymbol{F}_{RC} + \boldsymbol{F}_{det} \tag{6}$$

The detergent-phase model structure factor must be calculated now at absolute scale. This is made by dividing the detergent-phase model into small volumes δv of uniform scattering length density ρ_{det}, corresponding to the pixels of the model density map, and by applying relation 1 with a total scattering length B_i of each volume δv given by

$$B_i = \rho_{det}\delta v \tag{7}$$

The volume δv of a pixel was about 5 Å^3 and the scattering length density of the detergent phase estimated on the assumption that it is 100% pure detergent. The solvent was assumed to be detergent free. The best value of the volume is obtained by a systematic R-factor search. Finally, the contrast between detergent phase and solvent can also be systematically varied in order to determine the optimal value of this parameter.

The aim of step 3 of the refinement is also to put the detergent-phase structure determination on a quantitative basis as much as possible. It was observed that the parametric adjustments occurring during this final calculation do not produce major changes of the shape of the detergent-phase model as compared to what was obtained at the end of step 2.

Results and Discussion

R-Factor Variations and Histogram Analysis. The detergent-phase modeling and refinement produced a marked improvement of R-factor values (relation 2) at the two contrast levels, 40% and 100% D_2O, that we used in our calculations, as shown in Table III. That is due to the fact that, in these two cases, the contribution of the detergent to diffraction does not vanish. The final R-factor values range from about 30%

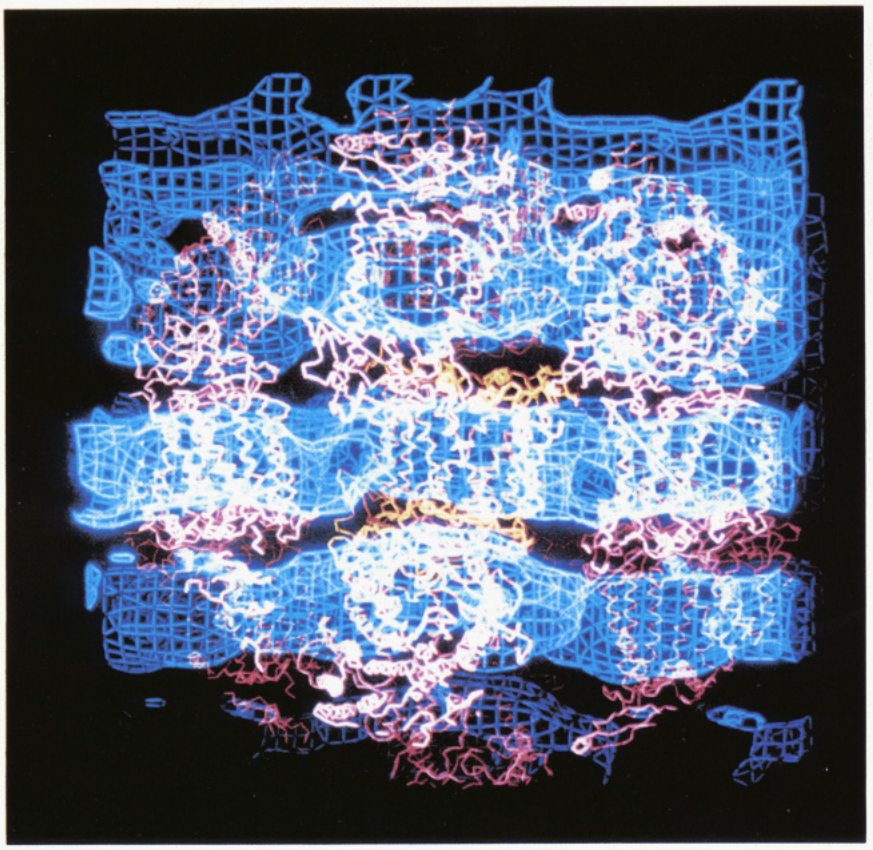

FIGURE 10: Detergent-phase structure in the crystal along the [010] direction. In the middle of the picture and parallel to the horizontal direction can be seen the alignment of a row of detergent rings along the [010] direction. The axis of these rings is vertical and also the axis (i.e., the transmembrane direction) of the RC molecules (pink and orange) which are surrounded by these rings.

to 40% and represent reasonably good results for low-resolution modeling. These values depend on the degree of smoothing of the three-dimensional detergent-phase model. Let us recall that the aim of the smoothing is to regularize the shape of the detergent phase.

The result of the search of best *R*-factor during step 3 calculations is illustrated on Figures 4 and 5. The optimal value of f_{det}, the volume fraction of the detergent phase in the unit cell, seems to range somewhere between 18% and 26% for a smoothed or unsmoothed model, respectively (Figure 4). This determination is not very accurate and depends somewhat on the modeling.

As far as the contrast between the detergent phase and solvent is concerned, Figure 5 shows that the optimal value is close to the theoretical value at the two contrasts, 40% and 100%. The theoretical contrast evaluations having been made with the assumption that the solvent does not contain any detergent, and the detergent phase is devoid of any water (see Appendix), this result can be considered as a confirmation of the validity of this hypothesis.

A feature of the refinement of the structure by the BESF method is shown on Figures 6 and 7. These two pictures represent pixel density histograms of best density maps at 40% D_2O contrast: Figure 6 after step 1 of structure determination and Figure 7 at the end of the refinement process. In addition to the global histogram of these maps one can see, separately, the histograms of the density inside and outside the RC molecular envelope. Ideally, at this contrast level the density histogram inside this envelope should show a peak at the same position as the solvent peak (because protein and solvent have the same average scattering length density at this contrast), and the histogram of the density outside the envelope should show two peaks, one for solvent (the highest one) and another one for the detergent phase, on the negative abscissa side (detergent has negative contrast with respect to solvent at this contrast). It can be seen that after step 1 of structure determination the density distribution inside and outside the envelope is far from ideal but that the refinement produces an evolution of the density distribution tending toward ideality. The same can be observed in Figure 8, which shows the final density histograms in the 100% D_2O contrast map. The peaks corresponding to protein, detergent phase, and solvent are clearly separated.

Volume of Detergent per RC Molecule and Detergent Concentration. From the optimal value of f_{det}, the volume occupied by the detergent phase can be estimated to range between 70 000 and 100 000 Å^3 per RC molecule (there are four RC molecules per unit cell, and the volume of a unit cell is 1.58×10^6 Å^3). As the detergent phase seems to contain only β-OG molecules (see above) and as the volume of one β-OG molecule is 417 Å^3, it can be concluded that there are of the order of 205 ± 35 molecules of β-OG per RC molecule in these crystals. The volume of the protein alone (with chromophores) being nearly equal to 125 000 Å^3, the fraction of the volume of detergent in a single RC–detergent complex is therefore of the order of 0.40 ± 0.04.

These values may be compared to those determined by hydrodynamic or chromatographic methods for detergent bound to RC in micellar solutions. Unfortunately, RC-bound detergent has not yet been measured in a micellar solution of β-OG. Data are available, however, for several other detergents. In micellar solution, about 238 LDAO molecules are associated to one RC and the fraction of volume occupied by the detergent in the whole RC–detergent complex is 0.45 (from Rivas et al., 1980; data recalculated for the true values of the RC polypeptide molecular weights). For dodecyl octaethylene

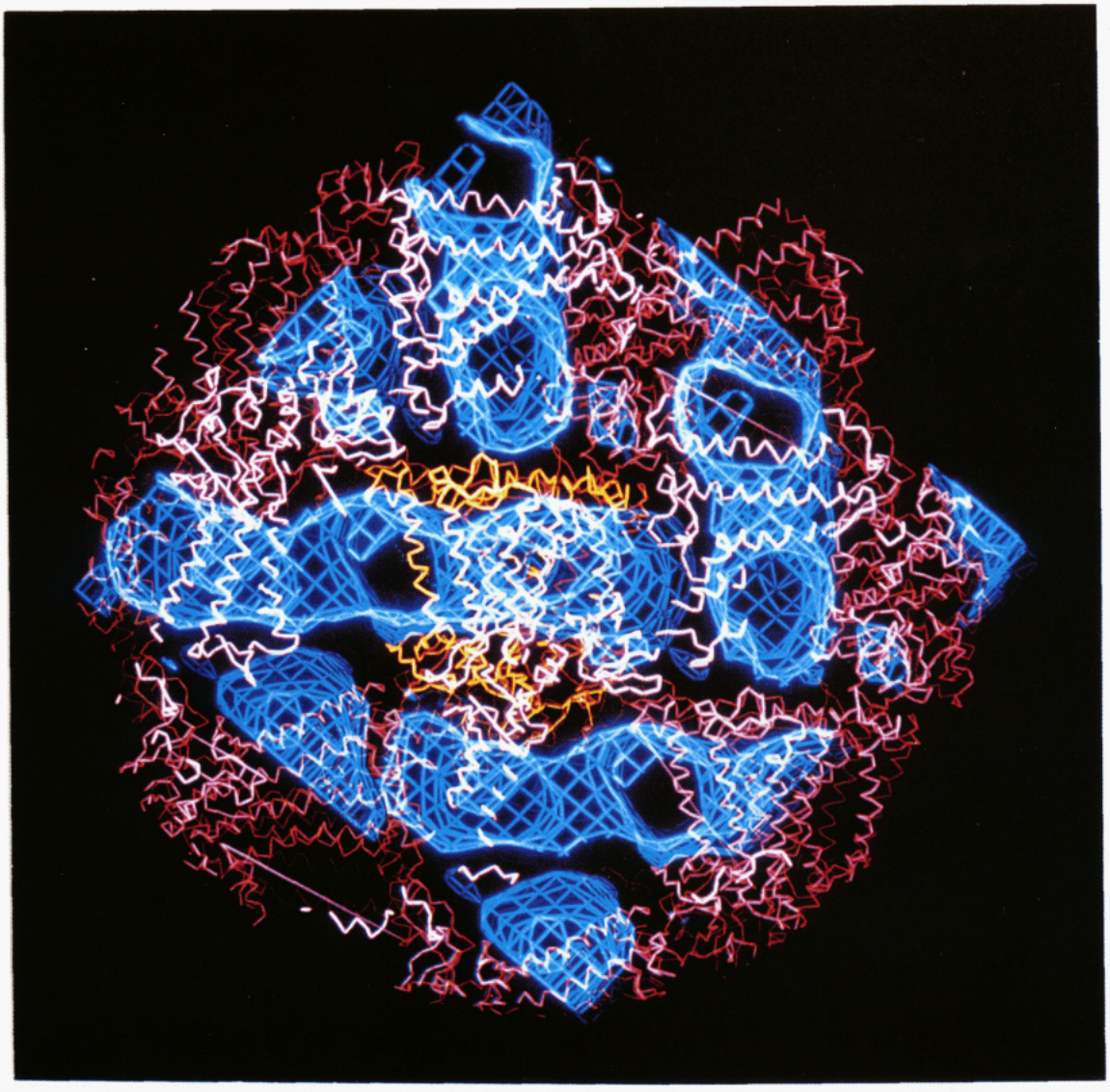

FIGURE 11: Same picture as Figure 10 but viewed down the [010] direction. This view is obtained by a 90° rotation of Figure 10 around a vertical axis. The horizontal direction in the plane of the figure is now parallel to [101].

glycol monoether and dodecyl maltoside (Moller and le Maire, unpublished) the volume fractions are respectively 0.46 and 0.41. These fractional volumes are rather similar to that found for β-OG associated to RC in the crystalline state. This seems to indicate that, during crystallization, the detergent–RC complexes are added to the growing crystal like individual building blocks, without major modification of the bound detergent/RC ratio.

Structure of the Detergent Phase and Detergent–Protein Interactions. The results of the structure determination of the detergent phase in *Rb. sphaeroides* crystals are shown in Figures 9–13. The detergent phase forms rings, which surround the protein and prosthetic groups at the level of the transmembrane α helices as is the case for LDAO in *Rps. viridis* RC crystals (Roth et al., 1989). Each ring is connected to two next-neighbor rings (Figure 10). The RC molecules corresponding to the connected rings are aligned along the 2_1 screw axes parallel to the *b* axis of the $P2_12_12_1$ unit cell. They form linear [010] chains without any connection between the chains. The plane of the rings in a chain is approximately parallel to, alternatively, (101) and (010) planes (Figure 11). In the X-ray diffraction pattern, the resolution of *Rb. sphaeroides* crystals is better in the *a* and *c* directions than in the *b* direction; this might be related to the existence of these chains of the detergent phase running along *b* (Arnoux et al., 1990), which may cause rows of molecules to slide relative to each other.

The size of a detergent-phase ring is about 70 Å along [010] and 50 Å in the other direction. The thickness of the detergent phase along the α helices is nearly 30 Å. These dimensions suggest that the detergent is organized like an ellipsoidal micelle around each RC, each micelle being connected by a bridge to the two next-neighbor micelles. In fact, the thickness of an anhydrous β-OG bilayer in the lamellar Lα phase is 23 Å, as calculated from X-ray diffraction data (Chung & Jeffrey, 1989; Ranck, personal communication). This is smaller than the thickness of 30 Å measured for the detergent phase along the α helices. Thus the detergent molecules are very likely oriented with their alkyl chains pointing toward the hydrophobic RC transmembrane regions, the polar head groups being located at the detergent phase/solvent interface (the external surface of the detergent phase; see Figure 12); all detergent molecules are in contact with the protein, in a monolayer type of arrangement.

As shown on Figure 9 by the color coding of the amino acid residues, the interaction between the protein and detergent phase is clearly *hydrophobic* around the transmembrane regions of L, M, and H. The same is true for the interaction with the highly hydrophobic prosthetic groups located there. Evidence for *hydrophilic* contacts between the H subunit and

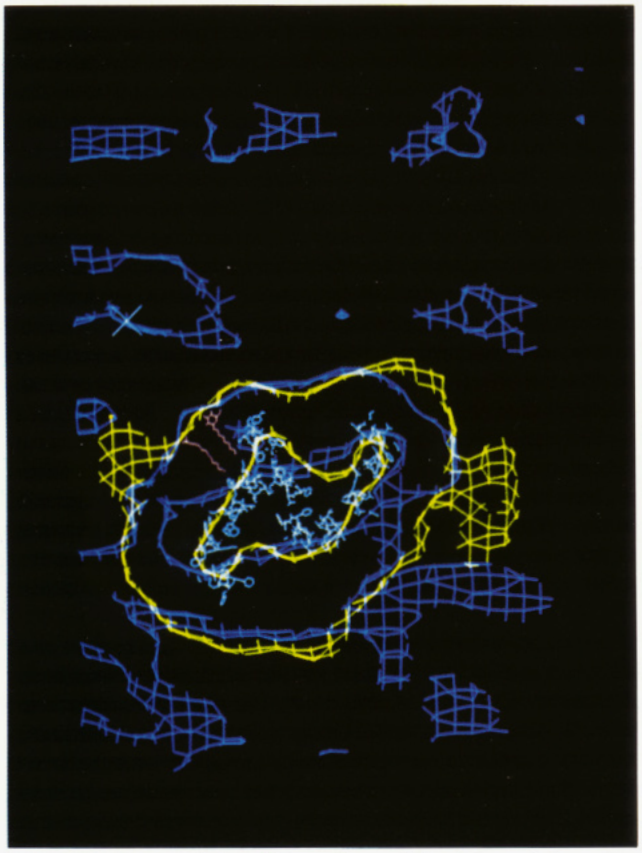

FIGURE 12: Superposition of the contours of the detergent-phase ring around *Rb. sphaeroides* (blue) and the ring around *Rps. viridis* (yellow), in the same equatorial plane of the two molecules. Inside the two contours we have arbitrarily placed two detergent molecules (in pink), with their polar head on the solvent side of the detergent phase and their hydrophobic tail pointing toward the hydrophobic transmembrane core of the RC molecule. It can easily be seen that the stretched length of both the β-OG and LDAO molecules is nearly equal to the detergent ring thickness in the equatorial plane.

the detergent phase is shown on Figure 9. Charged amino acid residues, namely, Asp H47, Asp H85, Arg H86, Lys H109, and Asp H110, located at the cytoplasmic surface of the H subunit, are found very close to the detergent-phase external surface of a neighbor chain. This is proof of the hydrophilic nature of the external surface of the detergent phase.

The structure of the detergent phase, found without any a priori model, and the details of its interaction with protein constitute direct proof of the existence of an amphiphilic micelle around the RC molecules which allows their solubilization in water.

Comparison with Rps. viridis. Figure 12 shows a superposition of the detergent phase existing around an RC molecule in *Rps. viridis* crystals on the detergent phase around an RC molecule of *Rb. sphaeroides* in the $P2_12_12_1$ unit cell. This was made by using the shifts and rotation operations appropriate for superposing an RC molecule from the *Rps. viridis* unit cell onto an RC molecule in the *Rb. sphaeroides* unit cell, calculated by using the homologous C_α atoms of L and M transmembrane helices (Arnoux et al., 1990). This superposition shows two main features:

(1) Around the transmembrane region of the RC molecules, the detergent rings are very similar. This quasi identity is certainly related to the fact that both detergent molecules have almost the same stretched length of about 15 Å omitting the H atoms (see Figure 14); the difference in the alkyl chain length is indeed compensated by the size of the polar group, which is greater for β-OG than for LDAO. Structural similarities between these two detergents are also found in the liquid-crystalline state, in the Lα phase at 25 °C. In this case the bilayer thickness is 23.5 Å for LDAO [calculated from data of Lawson et al. (1968) in D_2O and at 0.72 g of LDAO/g] and 23 Å for β-OG [calculated from data of Chung and Jeffrey (1989) and Ranck (personal communication)]. The crystallization of *Rps. viridis* RC molecules with LDAO (Michel, 1982) requires, however, the addition of a given amount of HPTH. This molecule may therefore be present in the detergent phase in these crystals as well. The structural role of this second amphiphile is not known. It was assumed (Deisenhofer & Michel, 1989a,b) that it contributes, by its small size, to the adaptability of the detergent phase to the molecular building in the crystal. It was recently shown (Timmins et al., 1991) that the size of the micelles (i.e., the value of their average radius of curvature) in a solution of LDAO + HPTH in water decreases as the concentration of HPTH increases. Within the limits of accuracy of our method, the comparison of the detergent rings of the two different RC systems does not reveal any feature which could be ascribed specifically to the presence of HPTH in the *Rps. viridis* RC crystals.

(2) The organization of the detergent phase in the neighborhood of the H subunit is completely different. This is due to the difference of molecular packing in the two systems. The space group is $P2_12_12_1$ for *Rb. sphaeroides* and $P4_32_12$ for *Rps. viridis*. In the latter, protein–protein contacts occur between H subunits of neighboring molecules on one side and between cytochrome subunits of different molecules on the other side. In *Rb. sphaeroides*, the packing involves contacts between the H subunit of one molecule and the top of the L and M subunits of a neighbor (Chang et al., 1986). The interactions between the H subunits of the RC molecules and the detergent phase are thus different in both systems.

Implications for the Membrane-Bound State. In the *Rb. sphaeroides* membrane, the RC is considered to be tightly associated with the B875 LHCI for optimal trapping of excitation energy. Models have been proposed for the possible arrangement of B875 LHCI (αβ) heterodimers around the RC, e.g., dodecamers (Zuber, 1990). In *Rps. viridis* membranes, photosynthetic units are arranged in two-dimensional ordered hexagonal arrays as was observed on electron micrographs (Miller, 1979; Stark et al., 1984). These pictures were interpreted as showing, per photosynthetic unit, one RC molecule surrounded by a ring of B1020 LHCI. No similar results have been evidenced in the case of *Rb. sphaeroides* (no ordered arrays of photosynthetic units seem to exist in these membranes). But a structural homology between B1020 and B875 LHCI complexes was inferred recently from a comparison of the primary sequences of the respective α and β polypeptides (Zuber, 1990). Although the homology is probably limited by the fact that B1020 LHCI is known to contain an extra γ polypeptide, it may be of interest to compare the model of the ring of B1020 LHCI-RC units (Stark et al., 1984) to our detergent–RC model.

This has been done in Figure 13 where the vertical lines represent in a very simplified manner the height and diameter of the B1020 LHCI assembly, taken from Stark et al. (1984). It can be seen that, in a direction parallel to the long diameter of the RC molecule, there is no space left between the presumed LHCI ring and the RC molecule. The detergent phase seems to be substituted here directly to the LHCI molecules. In a direction along the small diameter (not shown), there is a space left between the LHCI ring and the RC molecule, presumably occupied in the membrane by phospholipids. The detergent ring height is here smaller than in the first direction and is shorter than the transmembrane α helices. It appears

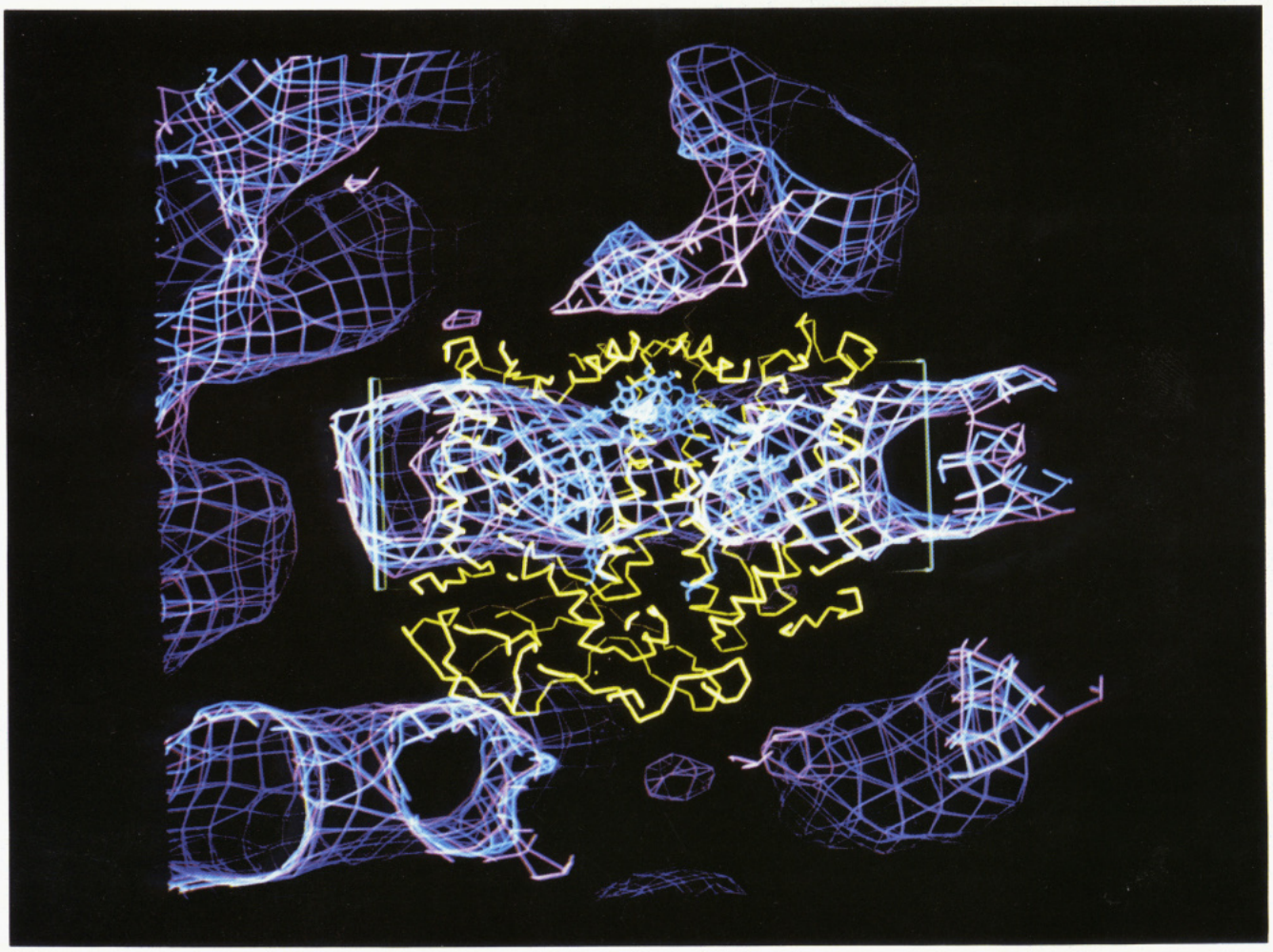

FIGURE 13: A view parallel to the long diameter of the RC molecule showing the cross section of the RC molecule (in yellow) with its chromophores (in light blue), the detergent ring (shown by two violet contours) and, very schematically, the presumed LHCI dodecamer ring (in green). Assuming that this LHCI model is correct, this picture shows that, along this diameter of the RC, the detergent phase replaces the LHCI molecules and not membrane phospholipids. (The two detergent-phase contours correspond to two different models, refined with a detergent volume of 70 000 and 100 000 Å^3 per RC molecule, respectively. The two contours are not very different.)

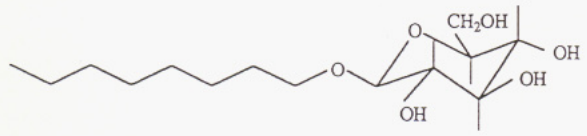

n-octyl β-D-glucoside (β-OG)

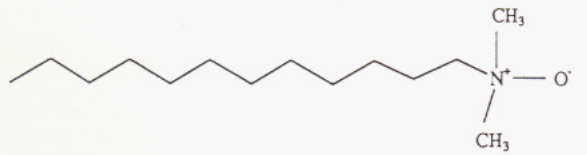

lauryldimethylamine oxide (LDAO)

FIGURE 14: Schematic representation without H atoms of stretched LDAO and β-OG molecules.

Table IV			
molecule type	b ($\times 10^{-12}$ cm)	V (Å^3)	N^a (mol/L)
H_2O	−0.179	30	
D_2O	1.877	30	
NaCl	1.341	24[b]	0.24
PEG[c]	0.387	60[d]	3.07[e]
β-OG	2.132 + 4.112 C[f]	417[g]	

[a] Number of moles in the solvent. [b] Molecular volume calculated for a solution of 0.24 mol/L NaCl in water (refer to the *Handbook of Chemistry*, 61st ed.). [c] Per monomeric unit (CH_2CH_2O). [d] Atha and Ingham (1981); Zulauf et al. (1985). [e] i.e., 135 g/L. [f] Assuming that β-OG has four labile H atoms. [g] Reynolds (1985).

thus that the detergent–protein interaction found in the crystal is very likely a substitute for different types of molecular interactions in vivo.

Detergent and Crystallization. Three main conclusions may be drawn from these results concerning the process of crystallization of these membrane proteins with detergent:

The similarity observed between β-OG and LDAO rings around the RC molecules seems to indicate that the length of the detergent molecule is one of the molecular parameters of primary importance. This confirms the known experimental result that, within a given detergent series, these RC molecules crystallize only with a detergent molecule of a given alkyl chain length, 12 (CH_2)(LDAO) and 8 (CH_2)(β-OG) for RC from *Rps. viridis* and *Rb. sphaeroides*, respectively.

The ability of the detergent to form variable curvature interfaces in water solvent seems to be another prerequisite for crystallization, as suggested by an examination of the curvature of the surface of the detergent phase. As shown by Chung and Jeffrey (1989), β-OG is able to form cylindrical and cubic phases with water at room temperature. The same is true for LDAO (Lawson et al., 1968). Addition of amphiphilic molecules like HPTH may contribute to local adaptation of the curvature to the protein geometry.

The present study shows thirdly that the packing energy of the membrane protein crystal is a function of three types of interaction. The protein–protein interaction defined by the direct protein–protein contacts is very likely the primary term, because without protein–protein contacts, long-range atomic

order would hardly be possible. The second type of interaction is the detergent phase–solvent surface energy, and it contributes to that packing energy term by the intermicellar bridges. Finally, the detergent phase and the protein have also "external" interactions, that is to say, interactions which are not located in the transmembrane region of the protein. These interactions involve the H subunit of one RC molecule and the detergent ring of a neighbor RC–detergent complex and contribute thus for a third term to the packing energy. This does imply that in the crystallization process the detergent has not only the passive role of solubilizing the protein by an ad hoc coverage of the hydrophobic regions but also an active role in the condensation of each individual detergent–RC complex onto the crystal, by a definite contribution to the packing energy.

ACKNOWLEDGMENTS

We are very grateful to Dr. M. le Maire and Dr. J. L. Ranck, Centre de Gênêtique Moléculaire, CNRS, Gif-sur-Yvette, France, and to Dr. J. V. Moller, Biophysics Institute, Aarhus University, Denmark, for providing us with unpublished data.

APPENDIX: SCATTERING LENGTH DENSITY CALCULATIONS

Scattering Length Density of the Solvent $\rho_{solvent}$. The scattering length density of the solvent is given by

$$\rho_{solvent} = (N_w b_w + N_{NaCl} b_{NaCl} + N_{PEG} b_{PEG} + N_{OG} b_{OG})\mathcal{N} \quad (A1)$$

as a function of $\mathcal{N}$, the Avogadro number, and b_w, the scattering length of a water molecule, given by the relation

$$b_w = b_{H_2O} + (b_{D_2O} - b_{H_2O})C$$

where C is the relative concentration of D_2O molecules in the water ($H_2O + D_2O$) in the system, b_{NaCl}, the scattering length of a NaCl molecule, b_{PEG}, the scattering length of a PEG monomer, b_{OG}, the scattering length of a β-OG molecule, and the corresponding molar concentrations N_w, N_{NaCl}, N_{PEG}, and N_{OG} in the solvent. The relation of conservation of volume

$$(N_w V_w + N_{NaCl} V_{NaCl} + N_{PEG} V_{PEG} + N_{OG} V_{OG})\mathcal{N} = V_0 \quad (A2)$$

where V_0 is unit volume and V_w, V_{NaCl}, V_{PEG}, and V_{OG} are the volumes of the different molecules in the solvent allows an estimate of the value of N_w.

Scattering Length Density of the Detergent-Rich Phase ρ_{det}. In the same way, the scattering length density of the detergent-rich phase is given by

$$\rho_{det} = (N'_w b_w + N'_{OG} b_{OG})\mathcal{N} \quad (A3)$$

where N'_w and N'_{OG} are the molar concentrations of water and detergent in the phase and are related by

$$(N'_w V_w + N'_{OG} V_{OG})\mathcal{N} = V_0 \quad (A4)$$

Isopycnic Scattering Length Density Point of the Detergent-Rich Phase. The D_2O concentration C_m corresponding to zero contrast between detergent and solvent is given by the equation:

$$\rho_{det} = \rho_{solvent} \quad (A5)$$

Assuming that N_{OG} and $N'_w \approx 0$, one finds $C_m \approx 16\%$. The exact values of N_{OG} and N'_w are not known.

The numerical values used are shown in Table IV.

Registry No. β-OG, 29836-26-8.

REFERENCES

Arnoux, B., Ducruix, A., Reiss-Husson, F., Lutz, M., Norris, J., Schiffer, M., & Chang, C. H. (1989) *FEBS Lett. 258*, 47–50.

Arnoux, B., Ducruix, A., Astier, C., Picaud, M., Roth, M., & Reiss-Husson, F. (1990) *Biochimie 72*, 525–530.

Atha, D. H., & Ingham, K. C. (1981) *J. Biol. Chem. 256*, 12108–12117.

Blow, D. M., & Crick, F. H. C. (1959) *Acta Crystallogr. 12*, 794–802.

Chang, C. H., Tiede, D., Tang, J., Smith, U., Norris, J., & Schiffer, M. (1986) *FEBS Lett. 205*, 82–86.

Chung, Y. J., & Jeffrey, G. A. (1989) *Biochim. Biophys. Acta 985*, 300–306.

Deisenhofer, J., & Michel, H. (1989a) *EMBO J. 8*, 2149–2170.

Deisenhofer, J., & Michel, H. (1989b) *Science 245*, 1463–1473.

Ducruix, A., & Reiss-Husson, F. (1987) *J. Mol. Biol. 193*, 419–421.

Ducruix, A., Arnoux, B., & Reiss-Husson, F. (1988) in *The photosynthetic reaction center: structure and dynamics* (Breton, J., & Vermeglio, A., Eds.) pp 21–25, Plenum Press, New York.

Herrmann, K. W. (1962) *J. Phys. Chem. 66*, 295–300.

Jacrot, B. (1976) *Rep. Prog. Phys. 39*, 911–953.

Lawson, K. D., Mabis, A. J., & Flautt, T. J. (1968) *J. Phys. Chem. 72*, 2058–2065.

Le Maire, M., Kwee, S., Andersen, J. P., & Moller, J. V. (1983) *Eur. J. Biochem. 129*, 525–532.

Michel, H. (1982) *J. Mol. Biol. 158*, 567–572.

Osborne, H. B., Sardet, C., Michel-Villaz, M., & Chabre, M. (1978) *J. Mol. Biol. 123*, 177–206.

Ray, W. J., & Puvathingal, J. (1985) *Anal. Biochem. 146*, 307.

Reynolds, J. (1985) *Methods Enzymol. 117*, 41.

Rivas, E., Reiss-Husson, F., & Le Maire, M. (1980) *Biochemistry 19*, 2943–2950.

Roche, C. T., Strauss, M. G., & Brenner, R. (1985) *IEEE Trans. Nucl. Sci. 32*, 373–379.

Roth, M. (1986) *Acta Crystallogr. A42*, 230–240.

Roth, M. (1987) *Acta Crystallogr. A43*, 780–787.

Roth, M. (1990) Crystallographic Computing School, Bischenberg, France (in press).

Roth, M., & Lewit-Bentley, A. (1986) *J. Phys. 47* (C5), 27–34.

Roth, M., Lewit-Bentley, A., & Bentley, G. A. (1984) *J. Appl. Crystallogr. 17*, 77–84.

Roth, M., Lewit-Bentley, A., Michel, M., Deisenhofer, J., Huber, R., & Oesterhelt, D. (1989) *Nature 340*, 659–661.

Sardet, C., Tardieu, A., & Luzzati, V. (1976) *J. Mol. Biol. 105*, 383–407.

Stark, W., Kühlbrandt, W., Wildhaber, H., Wehrli, E., & Mühlethaler, K. (1984) *EMBO J. 3*, 777–783.

Timmins, P. A., Hauk, J., Wacker, T., & Welte, W. (1991) *FEBS Lett. 280*, 115–120.

Wang, B. C. (1985) *Methods Enzymol. 115*, 90–111.

Worcester, D. L., Gillis, J. M., O'Brien, E. J., & Ibel, K. (1976) *Brookhaven Symposium on Neutron Scattering in Biology* (Schoenborn, B., Ed.) Vol. III, pp 101–113, Brookhaven National Laboratory, Upton, NY.

Zuber, H. (1990) in *Molecular Biology of Membrane-Bound Complexes in Phototrophic Bacteria* (Drews, G., & Dawes, E. A., Eds.) pp 161–181, Plenum Press, New York.

Zulauf, M., Weckström, K., Hayter, J. B., Degiorgio, V., & Curti, M. (1985) *J. Phys. Chem. 89*, 3411–3417.